Title

Neuregulin-1/ErbB4 Signaling Regulates Visual Cortical Plasticity

Journal

Neuron, 92(1)

ISSN

0896-6273

Authors

Sun, Yanjun

Ikrar, Taruna

Davis, Melissa F

et al.

Publication Date

2016-10-01

DOI

10.1016/j.neuron.2016.08.033

Peer reviewed

HHS Public Access

Author manuscript

Neuron. Author manuscript; available in PMC 2017 February 15.

Published in final edited form as:

Neuron. 2016 October 05; 92(1): 160–173. doi:10.1016/j.neuron.2016.08.033.

Neuregulin-1 (NRG1)/ErbB4 signaling regulates visual cortical plasticity

Yanjun Sun[1], **Taruna Ikrar**[1], **Melissa F. Davis**[2], **Nian Gong**[3], **Xiaoting Zheng**[2], **Z. David Luo**[3], **Cary Lai**[4], **Lin Mei**[5], **Todd C. Holmes**[6], **Sunil P. Gandhi**[2], and **Xiangmin Xu**[1,7,8]

[1]Department of Anatomy and Neurobiology, School of Medicine, University of California, Irvine, CA 92697-1275, USA

[2]Department of Neurobiology and Behavior, University of California, Irvine, CA 92697- 4550, USA

[3]Department of Anesthesiology and Perioperative Care, University of California, Irvine, CA 92697-4265, USA

[4]Department of Psychological and Brain Sciences, Indiana University, Bloomington, IN 47405, USA

[5]Department of Neuroscience and Regenerative Medicine, Augusta University, Augusta, GA 30912, USA

[6]Department of Physiology and Biophysics, School of Medicine, University of California, Irvine, CA 92697- 4560, USA

[7]Department of Biomedical Engineering, University of California, Irvine, CA 92697-2715, USA

[8]Department of Microbiology and Molecular Genetics, University of California, Irvine, CA 92697-2715, USA

Summary

Experience alters cortical networks through neural plasticity mechanisms. During a developmental critical period, the most dramatic consequence of occluding vision through one eye (monocular deprivation) is a rapid loss of excitatory synaptic inputs to parvalbumin-expressing (PV) inhibitory neurons in visual cortex. Subsequent cortical disinhibition by reduced PV cell activity allows for excitatory ocular dominance plasticity. However, the molecular mechanisms underlying critical period synaptic plasticity are unclear. Here we show that brief monocular deprivation during the critical period down-regulates neuregulin-1(NRG1)/ErbB4 signaling in PV neurons, causing retraction of excitatory inputs to PV neurons. Exogenous NRG1 rapidly restores excitatory inputs onto deprived PV cells through downstream PKC-dependent activation and AMPA receptor exocytosis, thus enhancing PV neuronal inhibition to excitatory neurons. NRG1 treatment prevents the loss of deprived eye visual cortical responsiveness in vivo. Our findings reveal molecular,

[#]Address all manuscript correspondence to: Dr. Xiangmin Xu, Department of Anatomy and Neurobiology, School of Medicine, University of California, Irvine, CA 92697-1275 xiangmin.xu@uci.edu.

Author Contributions: Y.S., N.G. and X.X. performed molecular experiments, viral injection and animal preparations. T.I. performed electrophysiological recordings. D.F.M. and X.Z. performed *in vivo* imaging experiments. L.M. helped with experimental design and provided the loxP-flanked ErbB4 mice. C.L. provided the ErbB4 antibody. X.X., T.C.H., Y.S., S.P.G., and D.F.M. analyzed the data, wrote the manuscript and prepared the figures. X.X. designed and oversaw the project.

cellular and circuit mechanisms of NRG1/ErbB4 in regulating the initiation of critical period visual cortical plasticity.

Introduction

Synaptic plasticity of neural circuits is a required feature of learning, memory, and similar cognitive processes. Neural circuitry in the brain is shaped by experience, most profoundly during ‘critical periods’ in early postnatal life. Experience-dependent critical period plasticity has been extensively studied in the visual cortex (Hensch, 2005). Adjustments of excitatory and inhibitory synaptic strength are believed to be a major mechanism by which cortical networks adapt to sensory input over a range of timescales from seconds to days (D'Amour J and Froemke, 2015; Feldman, 2012; Ma et al., 2013; Maffei et al., 2010).

Changes in cortical inhibition exerted by inhibitory interneurons are essential for regulating the critical period of visual development. Recently, fast-spiking, parvalbumin-positive inhibitory neurons (referred to as PV neurons) have been identified as the initial locus for critical period cortical plasticity (Kuhlman et al., 2013). PV neurons are rapidly inhibited by visual deprivation via monocular eyelid suture during the critical period, which is attributed to a decrease in local excitatory circuit inputs onto these interneurons (Kuhlman et al., 2013). The initial and transient reduction of PV cell activity establishes the conditions necessary for the experience-dependent excitatory cortical plasticity (i.e., ocular dominance plasticity, ODP). While progress has been made to understand specific neuronal types in driving critical period plasticity, the molecular mechanisms that translate brief sensory deprivation into functional changes in circuit connections remain unresolved.

Neuregulin-1 (NRG1) is essential for the normal development of the nervous system, and signaling through its tyrosine kinase receptor ErbB4 has been implicated in synaptic plasticity associated with long term potentiation (LTP)and GABAergic circuit development (Fazzari et al., 2010; Huang et al., 2000; Mei and Xiong, 2008; Woo et al., 2007). We tested whether NRG1/ErbB4 signaling regulates functional circuit connections of PV interneurons and excitatory neurons during the critical period of visual development. Here we show that NRG1/ErbB4 signaling rapidly controls excitatory synaptic inputs onto PV neurons and thus PV-cell mediated cortical inhibition in response to visual deprivation. Our study establishes molecular, cellular and circuit mechanisms of NRG1/ErbB4 in regulating the initiation of critical period visual cortical plasticity.

Results

NRG1/ErbB4 signaling in PV neurons is rapidly reduced by visual deprivation

To determine how sensory experience is transduced into a loss of excitatory inputs to fast-spiking interneurons, we examined developmental expression and experience-dependent regulation of NRG1/ErbB4 signaling. We focused on layer 2/3 (L2/3) PV neurons in the binocular zone of mouse primary visual cortex (V1), where a reduction in PV cell firing rates and disinhibition of upper layer excitatory neurons occurs during the initial stage of critical period ocular dominance plasticity. To genetically label PV neurons, PV-IRES-Cre

mice (Hippenmeyer et al., 2005) were crossed with Ai9 tdTomato reporter mice (Madisen et al., 2010).

NRG1 and ErbB4 expression in PV neurons is developmentally regulated. ErbB4 expression in the visual cortex precedes PV expression (Fig. 1A-C). PV neurons show strong ErbB4 expression during the critical period of mouse visual development, as defined by ocular dominance plasticity. The ErbB4 expressing cells form a major subset of GABAergic neurons in visual cortex (Fig. S1). NRG1 expression in the brain has been mapped using *in situ* hybridization (Liu et al., 2011); however, no studies have determined if PV inhibitory neurons express NRG1. To determine this, we performed NRG1 immunostaining in visual cortical sections. PV neurons have strong and concentrated NRG1 expression revealed by immunostaining; this distinguishes them from surrounding putative excitatory neurons (Fig. 1D). The stronger expression of NRG1 by PV neurons is confirmed with cell specific fsTRAP analysis (Fig. S2); the NRG1 mRNA expression in PV neurons of normal mice is on average 170 fold higher as compared with excitatory neurons targeted by using Emx1-Cre mice. Importantly, the developmental expression of NRG1 in PV cells peaks at the critical period peak and correlates with the time course of critical period ocular dominance plasticity in mouse visual cortex (Fig. 1A-B, D-E).A great majority of PV neurons are immunopositive for NRG1. The average percentage of NRG1-expressing PV cells in L2/3 of mouse V1 is 92.5% during the critical period peak. The co-expression of the ligand NRG1 and its receptor ErbB4 in PV neurons may allow these neurons to regulate their synaptic plasticity through activity-dependent NRG1/ErbB4 signaling.

Consistent with our previous finding that firing rates of PV neurons in binocular visual cortex are rapidly inhibited with 1-day monocular deprivation (Kuhlman et al., 2013), visual deprivation reduces NRG1 expression for both mRNA (Fig. 2A, B) and protein levels (Fig. 2C-D) in PV neurons. Monocular deprivation also decreases the levels of activated ErbB4 (as measured by phospho-specific ErbB4 immunostaining) and overall phosphotyrosine levels in PV neurons (Fig. 2C-D, G-I). In contrast, brief visual deprivation has no effect on NRG1 expression in putative excitatory neurons (Fig. 2J).Thus the acute and selective down-regulation of NRG1 signaling in PV neurons induced by sensory deprivation is a candidate for the molecular basis of the rapid retraction of excitatory inputs to these cells and their reduced spiking activity. To further address the activity-dependent control of NRG1 expression by PV neurons, we functionally mimicked monocular deprivation effects by using Designer Receptors Exclusively Activated by Designer Drugs (DREADDs) (Sternson and Roth, 2014) to inhibit PV neuronal activity *in vivo* for 24 hours. We find that reduced PV neuronal activity evoked by 24 hour DREADDs treatment phenocopies the decreased NRG1 expression in the same targeted cells seen after 24 hours of monocular deprivation (Fig. 2F, K).To determine whether ErbB4 activation is important for NRG1 expression in PV neurons, we acutely treated the mouse cortex with an ErbB receptor tyrosine kinase inhibitor AG1478 for less than 24 hours through intracerebroventricular injection. ErbB receptor inhibition decreases NRG1 expression in PV neurons in AG1478 treated animals (Fig. 2L).

We reasoned that exogenous NRG1 treatment should reverse the physiological impact of visual deprivation on PV cells. As shown in Fig. 2, NRG1/ErbB4 signaling in deprived PV cells in visual cortex is up-regulated through exogenous NRG1 treatment via subcutaneous

administration of recombinant NRG1 containing only the EGF core domain of NRG1-β1. This form of NRG1 has been shown previously to penetrate the blood–brain barrier and functionally activate ErbB4 in the cortex (Abe et al., 2011). Exogenous NRG1 treatment results in significantly increased immunostaining of NRG1, and increased phosphorylation of ErbB4 and protein tyrosine phosphorylation in PV cells in binocular visual cortex despite monocular deprivation (Fig. 2E, G-I). These findings indicate that systemic administration of NRG1 can be used to override the effects of monocular deprivation and independently manipulate NRG1 signaling in visual cortex to test functional outcomes *in vivo*.

Exogenous NRG1 restores excitatory input to deprived PV neurons

To examine the causal link between decreased NRG1 signaling and the loss of excitatory inputs to PV cells, we tested the effects of NRG1 treatment on PV cell inputs following visual monocular deprivation. We predicted that enhancing NRG1 signaling would enhance excitatory inputs to deprived PV cells in layer (L) 2/3 of visual cortex. We measured the connectivity strength and laminar distribution of presynaptic excitatory inputs onto L2/3 PV neurons in brain slices taken from binocular visual cortex of critical period mice (P27-P30) using laser scanning photo stimulation (LSPS) via glutamate uncaging (Kuhlman et al., 2013; Xu et al., 2016) (Fig. 3A, Fig. S3). The LSPS approach is effective for detailed local circuit mapping. It involves first recording from a single neuron, then sequentially stimulating at surrounding sites to evoke action potentials from neurons in those sites through spatially restricted optically evoked glutamate release; recording from the potential postsynaptic neuron allows one to determine if there is actual synaptic input from that particular site. Physiological mapping experiments were performed in both normal and deprived mouse V1 slices. Normal PV neurons receive strong local excitatory inputs from L4 and upper L5 and as well as from L2/3; their inputs are dramatically reduced following 1-2 day monocular visual deprivation (Kuhlman et al., 2013) (Fig. 3B-D).

To test our prediction that enhancing NRG1 signaling specifically enhances excitatory inputs to deprived PV cells, we examined whether enhanced NRG1 signaling restores normal excitatory drive onto these PV cells. Exogenous NRG1 treatment does not alter resting membrane potential or intrinsic membrane excitability in PV cells under normal or monocular deprivation conditions (Fig. S4; Table S1); thus intrinsic neuronal properties are not the locus for NRG1 effects. Further, acute bath application of recombinant NRG1 does not significantly modulate local excitatory synaptic inputs or direct uncaging responses of control PV neurons in binocular V1 of normal, non-lid sutured PV-Cre;Ai9 mice (Fig. 3B, C, K). This suggests that NRG1 signaling is sufficiently high to maintain synaptic input to normal PV neurons during the critical period. In contrast, bath NRG1 rapidly increases the amplitude of excitatory synaptic input to 1-2 day deprived PV cells (Fig. 3D-G, J; Table S2). Bath applied NRG1 greatly potentiates direct glutamate evoked responses as measured by responses to uncaging at perisomatic regions of PV cells. The NRG1 effects on direct responses are similar with and without the co-application of tetrodotoxin (TTX) that blocks evoked synaptic inputs (Fig. 3K; Fig. S5). These NRG1 enhanced responses are supported by previous studies (Abe et al., 2011; Tamura et al., 2012) and further confirmed by the finding that NRG1 treatment increases glutamate evoked spiking in monocular deprived PV neurons (Fig. S6).Bath NRG1 effects are robust with a fast time course (Fig. 3G). The

NRG1 response increases observed are clearly detectable within 10 minutes and reach a plateau around 20 minutes following NRG1 bath application. NRG1 potentiation persists with long duration in the continued presence of the peptide, but its effects are quickly and completely eliminated within 30 minutes of washout.

The excitation-enhancing effects of NRG1 on deprived PV neurons are concentration dependent. We chose 5 nM bath NRG1 for slice mapping experiments based on a calibrated dose-response curve. This concentration is consistent with the physiological range of cortical NRG1 concentration (Liu et al., 2011). Desensitization of bath applied NRG1 is not seen in recordings of longer duration; NRG1 potentiation is seen with repeated cycles of washout followed by NRG1 re-applications on the same deprived PV neurons. Thus, this indicates that NRG1 signaling strongly enhances glutamate mediated responsiveness to restore excitatory synaptic transmission in an acute fashion rather than by initiating a long lasting modulation process.

The effects of bath administered NRG1 on excitatory inputs to deprived PV neurons are also observed in recordings of brain slices from animals treated with subcutaneously administered recombinant NRG1 *in vivo*. Consistent with the fast time course of bath NRG1 effects, 1-day monocular deprived PV neurons show clear enhancement of excitatory input after 1 hour of in vivo NRG1 treatment (1 μg NRG1 per mouse, note the larger dose for this rapid acute effect *in vivo*) (Fig. 3H). Exogenous *in vivo* NRG1 treatment (0.5 μg NRG1 per mouse, 3 injections daily) during the duration of monocular deprivation prevents deprivation-induced excitatory input reduction in PV neurons (Fig. 3I). There are temporal limits to these effects: NRG1 injection *in vivo* restricted to the first 24 hour period after eye lid suture does not prevent 48 hour-deprivation induced excitatory input reduction (data not shown).

Consistent with the physiological changes evoked by monocular deprivation, the *in vivo* suppression of PV cell activity by DREADDs for 24 hours during the critical period causes a large reduction in local excitatory inputs (Fig. 4A-C). The DREADDs treatment inhibited PV neuronal activity for the same duration as provided by 1 day monocular deprivation. We then measured local excitatory inputs to DREADDs-inhibited PV neurons in cortical slices. As it is seen in PV neurons following brief monocular deprivation, bath NRG1 rapidly enhances excitatory synaptic input and direct glutamate evoked responses of DREADDs-inhibited PV cells (Fig. 4D-G). Together with the finding that reduced PV neuronal activity evoked by DREADDs leads to decreased NRG1 expression (Fig. 2F, K), the DREADDs experiments complement our experiments with monocular deprivation, and support our hypothesis that NRG1/ErbB4 signaling regulates excitatory inputs to physiologically inhibited PV neurons within the critical period.

To confirm the specificity of the effects of NRG1 on PV cells, we mapped the connectivity strength and laminar distribution of presynaptic excitatory inputs onto L2/3 excitatory pyramidal neurons in binocular visual cortex. NRG1 treatment does not modulate excitatory circuit inputs to pyramidal cells in normal or deprived animals as revealed by photostimulation mapping (Fig. 5). This is consistent with the finding that ErbB4 is not expressed in excitatory neurons in visual cortex (Fig. S1) (also see references (Fazzari et al.,

2010; Vullhorst et al., 2009)). Further, NRG1 treatment has no effect on intrinsic membrane excitability in pyramidal cells from normal or deprived animals (data not shown).In addition, the intracellular blocking experiments (see below, Fig. 6) further localize NRG1 effects to PV cells.

Downstream NRG1 signaling modulates PV responses

NRG1-induced enhancement of the deprived PV neuron response does not require NMDA receptor activation, as the co-application of NRG1 and a NMDA receptor antagonist, CPP (3-((R)-2-carboxypiperazin-4-yl)-propyl-1-phosphonic acid) has no effect of suppressing NRG1-enhanced PV neuronal responses (Fig. 6 A-B, I-J). As fast excitatory synaptic currents are mediated by postsynaptic AMPA receptors in PV neurons, this result also suggests that downstream NRG1 signaling modulates AMPA receptors.

The observed enhancement of PV excitatory inputs when NRG1 is administered is specific to direct NRG1 signaling at ErbB4 receptors on PV neurons. In the presence of an acutely applied ErbB receptor tyrosine kinase inhibitor AG1478, no significant NRG1 effects are observed for deprived PV cells (Fig.6 C-D, I-J). In PV-Cre; ErbB4$^{flx/flx}$ mice in which ErbB4 is ablated specifically in PV-positive interneurons (Long et al., 2003), bath NRG1 has no effect on excitatory synaptic inputs to monocular deprived PV neurons (Fig. S7 A-C). In addition, the PV cells with ErbB4 genetic ablation show reduced excitatory inputs compared with normal, non-ErbB4 knockout PV cells (Fig. S7 D-E). This result is in agreement with the previous finding that postsynaptic ErbB4 expression is important for the formation of excitatory synapses on hippocampal GABAergic interneurons (Fazzari et al., 2010).

Protein kinases are necessary for ocular dominance shifts during monocular deprivation (Berardi et al., 2003). We therefore tested whether NRG1-enhanced AMPA receptor responses by downstream NRG1/ErbB4 signaling require protein kinase C (PKC)-dependent activation. Protein phosphorylation of AMPA receptors is known to modulate AMPA receptor conductance, and the membrane trafficking and redistribution of AMPA receptors to the postsynaptic membranes (Lu et al., 2001).Canonical NRG1–ErbB signaling pathways often involve ERK and PI3K/Akt; many studies show that PI3K is an upstream regulator of protein kinase C (PKC) (Bekhite et al., 2011; Frey et al., 2006). It is also known that the downstream signals linked to ErbB include the phospholipase C-dependent PKC pathway (Mei and Xiong, 2008).To specifically restrict the inhibition of PKC activation in recorded PV neurons, we included a pseudosubstrate non-membrane permeable peptide inhibitor of protein kinase C (PKC 19-36) in recording glass pipettes (Chen et al., 2000) and measured the response to bath applied NRG1. Cellular inhibition of PKC through intracellular application of the PKC inhibitor blocks NRG1-induced responses (Fig. 6 E-F, I-J).Therefore, PKC activation is essential for NRG1/ErbB4 enhancement of AMPA receptor responses.

The timing of NRG1 potentiation of glutamate evoked responses is consistent with the rapid insertion of the intracellular pool of AMPA receptors and increased clustering of AMPA receptors (Lu et al., 2001) at the membrane surface of PV neurons. To determine if membrane-fusion dependent exocytosis of internal AMPA receptors is required for the NRG1 effects on deprived PV neurons, we included botulinum toxin light chains (BTX) in the recording pipette (Li et al., 2005). BTX blocks the exocytosis of postsynaptic vesicles

that contain new AMPA receptors, thus preventing membrane insertion. Using this approach, we determined whether BTX treatment blocks the effects of bath applied NRG1. In support of our hypothesis, intracellular application of BTX prevents the NRG1-induced enhancement of glutamate responses (Fig. 6 G-H, I-J). Thus NRG1 enhancement of PV excitatory inputs requires insertion of additional AMPA receptors in PV postsynaptic membrane surface.

To investigate the possible requirement of protein synthesis in NRG1-enhanced PV neuronal responses, we incubated cortical slices in a protein synthesis inhibitor, anisomycin (Huber et al., 2000) before bath NRG1 experiments. Compared to control experiments, blocking new protein synthesis by the anisomycin treatment does not appear to affect the potentiation of NRG1 on excitatory inputs to deprived PV neurons (data not shown). This result indicates that acute effects of bath administrated NRG1 do not require new protein synthesis.

NRG1 enhances cortical inhibition

Previous work showed that NRG1 increases evoked GABA release and modestly enhances inhibition onto excitatory neurons in prefrontal cortex and hippocampus (Tamura et al., 2012; Wen et al., 2010; Woo et al., 2007). However the mechanism of action of NRG1 on GABAergic neurons required further investigation. We show here that NRG1 strongly modulates evoked synaptic inhibition to pyramidal neurons in visual cortical slices, and this modulation depends both on sensory experience (i.e., monocular deprivation-dependent) and ErbB4 signaling (Fig. 7A-C). Bath NRG1 increases evoked inhibitory postsynaptic currents (IPSCs) to monocular deprived but not normal pyramidal neurons in visual cortex of wild type mice. In addition, NRG1 has no effect on evoked IPSCs in PV-Cre; ErbB4$^{flx/flx}$ mouse cortex.

We examined further if NRG1 modulates PV neuron-mediated postsynaptic responsiveness in excitatory neurons or the strength of PV inhibitory output connections to excitatory neurons by optogenetically evoking PV inhibitory inputs to pyramidal neurons (Fig. 7 D-G; Fig. S8). The experiments were performed in brain slices with Cre-directed channelrhodopsin-2 (ChR2) expression in PV neurons that synapse on pyramidal neurons (Madisen et al., 2012).Direct inhibitory connections to pyramidal neurons were mapped by ChR2 photoactivation of somatic spiking of presynaptic PV inhibitory neurons (Fig. S8F). Bath NRG1 application does not modulate PV specific inhibition to L2/3 pyramidal cells (Fig. 7 H-K). Thus the NRG1 increase of cortical inhibition in deprived cortex is localized specifically to enhance excitatory drive to deprived PV neurons, rather than modulating PV postsynaptic responsiveness or PV inhibitory synaptic connections to pyramidal cells.

Enhanced NRG1 signaling suppresses cortical plasticity

Next, we investigated the function of NRG1/ErbB4 signaling in ocular dominance plasticity *in vivo*. As described above and proposed in our model (Fig. 8A), down-regulation of NRG1 signaling following visual deprivation reduces excitatory inputs to PV neurons and subsequent inhibition onto excitatory neurons. Considering that enhancing inhibition prevents ocular dominance plasticity during the critical period (Kuhlman et al., 2013; Ma et al., 2013), we tested the hypothesis that enhancing NRG1/ErbB4 signaling in the cortex

through systemic NRG1 administration will suppress ocular dominance plasticity (Fig. 8B). To measure this plasticity, we determined the strength of eye-specific visual responses before and after four days of monocular deprivation using intrinsic signal optical imaging (Davis et al., 2015; Kalatsky and Stryker, 2003; Southwell et al., 2010) (Fig. 8C-D). We assessed ocular dominance shifts in wild type C57BL/6 mice treated subcutaneously with NRG1 versus saline following deprivation. In support of our hypothesis, the enhancement of NRG1 signaling (verified by post hoc immunostaining) strongly reduces ocular dominance plasticity (Fig. 8E left). To further test the role of ErbB4 signaling in ocular dominance plasticity, we performed imaging experiments before and after four days of monocular deprivation (without NRG1 treatment) using the PV-Cre; ErbB4$^{flx/flx}$ mice, and found that critical period plasticity is impaired in animals with PV specific ablation of ErbB4 receptors (Fig. 8E right).

A hallmark of ocular dominance plasticity during the critical period is the selective reduction of deprived eye visual cortical responses. Enhanced NRG1 signaling blocks the reduction of deprived eye responses that typifies critical period plasticity (Fig. 8F-G). Further, we find that enhanced NRG1 signaling facilitates a gain of non-deprived eye responses (Fig. 8H). This resembles the feature of residual plasticity observed in adult animals after prolonged deprivation (Sato and Stryker, 2008; Sawtell et al., 2003).

Discussion

Although physiological aspects of visual cortical ocular dominance plasticity have been widely studied since the initial discoveries of Hubel and Wiesel more than 50 years ago, the description of underlying molecular mechanisms has lagged behind. Previous studies have identified that signaling through neurotrophins (nerve growth factor, and brain-derived neurotrophic factor), insulin-like growth factor-1 (IGF1), transcriptional control by OTX2, maturation of the extracellular matrix, and synapse formation molecules contribute to control visual cortical plasticity during the critical period (Gu et al., 2013; Huang et al., 1999; Pizzorusso et al., 2002; Sugiyama et al., 2008; Tropea et al., 2006). By leveraging our recent discovery that PV inhibitory neuron activity and local excitatory inputs to PV cells are uniquely affected by brief monocular deprivation during the critical period of visual development (Kuhlman et al., 2013), the present study defines a novel and critical role of NRG1/ErbB4 in the initiation of temporally sensitive visual cortical plasticity by establishing the molecular, cellular and circuit mechanisms of NRG1/ErbB4 signaling actions.

Our study demonstrates how activity-dependent molecular signaling and sensory experience interact to rapidly shape functional circuit connections in the cortex. It is widely accepted that the maturation of inhibitory circuits creates the conditions necessary for synaptic competition during critical period plasticity. But the developmental mechanism within inhibitory neurons that initiates the critical period has proven elusive. Our work provides evidence that supports a potential cell autonomous mechanism for NRG1/ErbB4 signaling in PV neuron development. We show that PV neurons express the ligand NRG1 and its receptor ErbB4 during visual cortical development, and that blocking ErbB4 activation with an ErbB inhibitor AG1478 decreases NRG1 expression in PV neurons. Consistent with the

activity dependent regulation of NRG1 expression elsewhere in the brain (Eilam et al., 1998; Ozaki et al., 2004), we show that monocular deprivation rapidly down regulates NRG1 expression and its downstream signaling in PV neurons within visual cortex. Visually evoked firing rates of PV neurons are reduced by half with 1-day monocular deprivation (Kuhlman et al., 2013). Thus PV neurons likely interface firing activity to regulation of NRG1 signaling so as to rapidly translate sensory deprivation into their excitatory input synaptic plasticity. To augment our interpretation of activity-dependent control of NRG1/ErbB4 signaling by PV neurons, we have used DREADDs to specifically reduce PV activity *in vivo* for 24 hours. The DREADDs-evoked suppression of PV neuron spiking decreases NRG1 expression and causes a reduction in local excitatory input to targeted PV neurons as seen in 1-day monocular deprivation. Thus we establish a mechanistic link between down regulation of NRG1/ErbB4 signaling by visual deprivation, and the subsequent reduction in PV cell activity that facilitates ocular dominance plasticity during the critical period. The developmental down-regulation in NRG1 signaling after the critical period further supports the notion that NRG1/ErbB4 signaling is critical to the initiation of juvenile ocular dominance plasticity. Our work suggests that therapeutic intervention of NRG1/ErbB4 signaling may be developed to help treat central vision disorders in children with amblyopia, as well as other critical period disorders.

We also identify a key synaptic and circuit mechanism through which visual deprivation controls AMPA receptor-mediated synaptic inputs to PV neurons and sensory-evoked recruitment of PV cell-mediated inhibition. Exogenous NRG1 rapidly restores normal excitatory drive onto PV cells and enhances cortical inhibition in deprived cortex. Due to the canonical organization of cerebral cortex, the synaptic and circuit mechanisms through which NRG1 regulates cortical inhibition in an experience dependent fashion are likely generalized across cortical regions. Our findings offer mechanistic insights for previous studies in the hippocampus showing that NRG1 does not alter electrically-evoked glutamatergic transmission at Schaffer collateral-CA1 synapses, but increases inhibition to CA1 pyramidal cells to suppress induction of long-term potentiation (Chen et al., 2010; Huang et al., 2000). As the extraordinarily large NRG1 potentiation is observed in deprived but not normal PV neurons in critical period visual cortex, we suspect that NRG1 regulates PV neuronal activity in other brain regions during different developmental stages in a varying and state-dependent manner.

In addition, we identify key components of the NRG1 intracellular signaling cascade for potentiation of excitatory inputs to PV neurons. Since NRG1 potentiation of deprived PV neuron responses does not require NMDA receptors, downstream NRG1/ErbB4 signaling modulation of fast excitatory synaptic transmission is coupled to AMPA receptor membrane targeting in PV neurons. Although multiple NRG1–ErbB signaling pathways are known (Iwakura and Nawa, 2013; Mei and Xiong, 2008), further studies are required to elucidate specific intracellular signaling mechanisms in modulating PV neuronal responses in visual cortex. Through intracellular blocking and other experiments, we demonstrate that downstream PKC activation is essential for NRG1/ErbB4 modulation of the AMPA receptor responses, and that acute NRG1 enhancement of PV excitatory inputs requires a membrane fusion–dependent exocytosis of AMPA receptors independent of new protein synthesis.

Defects in NRG1/ErbB4 signaling, and PV inhibitory neuronal deficits have been identified as schizophrenia risk factors (Lewis et al., 2005; Mei and Xiong, 2008). Increasing evidence supports the idea that schizophrenia is a neurodevelopment disorder (Rapoport et al., 2012). Schizophrenia has a typical age of onset in late adolescence to early twenties (Gogtay et al., 2011).As schizophrenia appears to result from brain developmental defects during defined postnatal temporal windows (Lewis and Levitt, 2002), our discovery linking NRG1/ErbB4 signaling in PV neurons to critical period plasticity provides new insights into the pathology of schizophrenia. PV neuronal dysfunction, and late adolescent and early adult onset of schizophrenia may be temporally contingent on NRG1/ErbB4 signaling defects in the relevant brain regions. Further understanding of NRG1 signaling in shaping cortical development may shed light on developmental and plasticity disorders of the neocortex.

Experimental Procedures

Animals

All experiment procedures and protocols were approved by the Institutional Animal Care and Use Committee of the University of California, Irvine. Unless specified otherwise, the mice were of both sexes between postnatal days 27 and 31 at the time of experimentation. Further details are described in Supplemental Experimental Procedures.

Immunohistochemistry

To stain tissue sections with antibodies, conventional fluorescent immunohistochemistry was performed as described previously (Xu et al., 2010). Further details including quantitative fluorescence image analysis are described in Supplemental Experimental Procedures.

Purification of mRNA from fs-TRAP mice, Western blotting, and quantitative PCR

Please see the details described in Supplemental Experimental Procedures.

Electrophysiology and Laser Scanning Photostimulation

Electrophysiological recordings and photostimulation via glutamate uncaging were performed as in reference (Kuhlman et al., 2013; Xu et al., 2016). PV specific inhibitory connections to excitatory neurons were mapped using laser scanning ChR2 photoactivation. Further details are described in Supplemental Experimental Procedures.

Transcranial Intrinsic Signal Optical Imaging

Mapping of the primary visual cortex using Fourier intrinsic signal optical imaging was performed through the intact skull (Davis et al., 2015). Further details are described in Supplemental Experimental Procedures.

Statistical analyses

All data are reported as mean ± standard error of the mean (SEM). When comparing two independent groups, normally distributed data were analyzed using a Student's t-test. In the case data were not normally distributed a Mann-Whitney U test was used. In the case more than 2 groups were compared and data were normally distributed, an ANOVA was

performed and followed by post-hoc comparisons when justified. In other cases, a non-parametric one-way ANOVA Kruskal Wallis test was used and followed by comparisons with Mann–Whitney U tests. A p value (≤ 0.05) was considered statistically significant.

Sample size n was defined as cell number, except in the case of quantitative immunochemical analysis and comparing the ocular dominance shift across treatments; n was defined as animal number or group.

Supplementary Material

Refer to Web version on PubMed Central for supplementary material.

Acknowledgments

We thank Dr. Joshua T. Trachtenberg for his suggestions on this manuscript. This work was supported by NIH grants NS078434 and MH105427 to X.X; a Searle Scholars award, Klingenstein Fellowship and a NIH grant EY024504 to S.P.G; and NIH grants GM102965, and GM107405 to T.C.H. This work was also made possible, in part, through access to the confocal facility of the Optical Biology Shared Resource of the Cancer Center Support Grant (CA-62203) at UC, Irvine.

References

Abe Y, Namba H, Kato T, Iwakura Y, Nawa H. Neuregulin-1 signals from the periphery regulate AMPA receptor sensitivity and expression in GABAergic interneurons in developing neocortex. J Neurosci. 2011; 31:5699–5709. [PubMed: 21490211]

Bekhite MM, Finkensieper A, Binas S, Muller J, Wetzker R, Figulla HR, Sauer H, Wartenberg M. VEGF-mediated PI3K class IA and PKC signaling in cardiomyogenesis and vasculogenesis of mouse embryonic stem cells. J Cell Sci. 2011; 124:1819–1830. [PubMed: 21540297]

Berardi N, Pizzorusso T, Ratto GM, Maffei L. Molecular basis of plasticity in the visual cortex. Trends Neurosci. 2003; 26:369–378. [PubMed: 12850433]

Chen C, Xu R, Clarke IJ, Ruan M, Loneragan K, Roh SG. Diverse intracellular signalling systems used by growth hormone-releasing hormone in regulating voltage-gated Ca2+ or K channels in pituitary somatotropes. Immunol Cell Biol. 2000; 78:356–368. [PubMed: 10947860]

Chen YJ, Zhang M, Yin DM, Wen L, Ting A, Wang P, Lu YS, Zhu XH, Li SJ, Wu CY, et al. ErbB4 in parvalbumin-positive interneurons is critical for neuregulin 1 regulation of long-term potentiation. Proc Natl Acad Sci U S A. 2010; 107:21818–21823. [PubMed: 21106764]

D'Amour J A, Froemke RC. Inhibitory and excitatory spike-timing-dependent plasticity in the auditory cortex. Neuron. 2015; 86:514–528. [PubMed: 25843405]

Davis MF, Figueroa Velez DX, Guevarra RP, Yang MC, Habeeb M, Carathedathu MC, Gandhi SP. Inhibitory Neuron Transplantation into Adult Visual Cortex Creates a New Critical Period that Rescues Impaired Vision. Neuron. 2015

Eilam R, Pinkas-Kramarski R, Ratzkin BJ, Segal M, Yarden Y. Activity-dependent regulation of Neu differentiation factor/neuregulin expression in rat brain. Proc Natl Acad Sci U S A. 1998; 95:1888–1893. [PubMed: 9465112]

Fazzari P, Paternain AV, Valiente M, Pla R, Lujan R, Lloyd K, Lerma J, Marin O, Rico B. Control of cortical GABA circuitry development by Nrg1 and ErbB4 signalling. Nature. 2010; 464:1376–1380. [PubMed: 20393464]

Feldman DE. The spike-timing dependence of plasticity. Neuron. 2012; 75:556–571. [PubMed: 22920249]

Frey RS, Gao X, Javaid K, Siddiqui SS, Rahman A, Malik AB. Phosphatidylinositol 3-kinase gamma signaling through protein kinase Czeta induces NADPH oxidase-mediated oxidant generation and NF-kappaB activation in endothelial cells. J Biol Chem. 2006; 281:16128–16138. [PubMed: 16527821]

Gogtay N, Vyas NS, Testa R, Wood SJ, Pantelis C. Age of onset of schizophrenia: perspectives from structural neuroimaging studies. Schizophr Bull. 2011; 37:504–513. [PubMed: 21505117]

Gu Y, Huang S, Chang MC, Worley P, Kirkwood A, Quinlan EM. Obligatory role for the immediate early gene NARP in critical period plasticity. Neuron. 2013; 79:335–346. [PubMed: 23889936]

Hensch TK. Critical period plasticity in local cortical circuits. Nat Rev Neurosci. 2005; 6:877–888. [PubMed: 16261181]

Hippenmeyer S, Vrieseling E, Sigrist M, Portmann T, Laengle C, Ladle DR, Arber S. A developmental switch in the response of DRG neurons to ETS transcription factor signaling. PLoS Biol. 2005; 3:e159. [PubMed: 15836427]

Huang YZ, Won S, Ali DW, Wang Q, Tanowitz M, Du QS, Pelkey KA, Yang DJ, Xiong WC, Salter MW, et al. Regulation of neuregulin signaling by PSD-95 interacting with ErbB4 at CNS synapses. Neuron. 2000; 26:443–455. [PubMed: 10839362]

Huang ZJ, Kirkwood A, Pizzorusso T, Porciatti V, Morales B, Bear MF, Maffei L, Tonegawa S. BDNF regulates the maturation of inhibition and the critical period of plasticity in mouse visual cortex. Cell. 1999; 98:739–755. [PubMed: 10499792]

Huber KM, Kayser MS, Bear MF. Role for rapid dendritic protein synthesis in hippocampal mGluR-dependent long-term depression. Science. 2000; 288:1254–1257. [PubMed: 10818003]

Iwakura Y, Nawa H. ErbB1-4-dependent EGF/neuregulin signals and their cross talk in the central nervous system: pathological implications in schizophrenia and Parkinson's disease. Frontiers in cellular neuroscience. 2013; 7:4. [PubMed: 23408472]

Kalatsky VA, Stryker MP. New paradigm for optical imaging: temporally encoded maps of intrinsic signal. Neuron. 2003; 38:529–545. [PubMed: 12765606]

Kuhlman SJ, Olivas ND, Tring E, Ikrar T, Xu X, Trachtenberg JT. A disinhibitory microcircuit initiates critical-period plasticity in the visual cortex. Nature. 2013; 501:543–546. [PubMed: 23975100]

Lewis DA, Hashimoto T, Volk DW. Cortical inhibitory neurons and schizophrenia. Nat Rev Neurosci. 2005; 6:312–324. [PubMed: 15803162]

Lewis DA, Levitt P. Schizophrenia as a disorder of neurodevelopment. Annu Rev Neurosci. 2002; 25:409–432. [PubMed: 12052915]

Li Q, Roberts AC, Glanzman DL. Synaptic facilitation and behavioral dishabituation in Aplysia: dependence on release of Ca2+ from postsynaptic intracellular stores, postsynaptic exocytosis, and modulation of postsynaptic AMPA receptor efficacy. J Neurosci. 2005; 25:5623–5637. [PubMed: 15944390]

Liu X, Bates R, Yin DM, Shen C, Wang F, Su N, Kirov SA, Luo Y, Wang JZ, Xiong WC, et al. Specific regulation of NRG1 isoform expression by neuronal activity. J Neurosci. 2011; 31:8491–8501. [PubMed: 21653853]

Livak KJ, Schmittgen TD. Analysis of relative gene expression data using real-time quantitative PCR and the 2(-Delta Delta C(T)) Method. Methods. 2001; 25:402–408. [PubMed: 11846609]

Long W, Wagner KU, Lloyd KC, Binart N, Shillingford JM, Hennighausen L, Jones FE. Impaired differentiation and lactational failure of Erbb4-deficient mammary glands identify ERBB4 as an obligate mediator of STAT5. Development. 2003; 130:5257–5268. [PubMed: 12954715]

Lu W, Man H, Ju W, Trimble WS, MacDonald JF, Wang YT. Activation of synaptic NMDA receptors induces membrane insertion of new AMPA receptors and LTP in cultured hippocampal neurons. Neuron. 2001; 29:243–254. [PubMed: 11182095]

Ma WP, Li YT, Tao HW. Downregulation of cortical inhibition mediates ocular dominance plasticity during the critical period. J Neurosci. 2013; 33:11276–11280. [PubMed: 23825430]

Madisen L, Mao T, Koch H, Zhuo JM, Berenyi A, Fujisawa S, Hsu YW, Garcia AJ 3rd, Gu X, Zanella S, et al. A toolbox of Cre-dependent optogenetic transgenic mice for light-induced activation and silencing. Nat Neurosci. 2012; 15:793–802. [PubMed: 22446880]

Madisen L, Zwingman Ta, Sunkin SM, Oh SW, Zariwala Ha, Gu H, Ng LL, Palmiter RD, Hawrylycz MJ, Jones AR, et al. A robust and high-throughput Cre reporting and characterization system for the whole mouse brain. Nature neuroscience. 2010; 13:133–140. [PubMed: 20023653]

Maffei A, Lambo ME, Turrigiano GG. Critical period for inhibitory plasticity in rodent binocular V1. J Neurosci. 2010; 30:3304–3309. [PubMed: 20203190]

Mei L, Xiong WC. Neuregulin 1 in neural development, synaptic plasticity and schizophrenia. Nat Rev Neurosci. 2008; 9:437–452. [PubMed: 18478032]

Ozaki M, Itoh K, Miyakawa Y, Kishida H, Hashikawa T. Protein processing and releases of neuregulin-1 are regulated in an activity-dependent manner. J Neurochem. 2004; 91:176–188. [PubMed: 15379898]

Pizzorusso T, Medini P, Berardi N, Chierzi S, Fawcett JW, Maffei L. Reactivation of ocular dominance plasticity in the adult visual cortex. Science. 2002; 298:1248–1251. [PubMed: 12424383]

Rapoport JL, Giedd JN, Gogtay N. Neurodevelopmental model of schizophrenia: update 2012. Mol Psychiatry. 2012; 17:1228–1238. [PubMed: 22488257]

Sato M, Stryker MP. Distinctive features of adult ocular dominance plasticity. J Neurosci. 2008; 28:10278–10286. [PubMed: 18842887]

Sawtell NB, Frenkel MY, Philpot BD, Nakazawa K, Tonegawa S, Bear MF. NMDA receptor-dependent ocular dominance plasticity in adult visual cortex. Neuron. 2003; 38:977–985. [PubMed: 12818182]

Smith SL, Trachtenberg JT. Experience-dependent binocular competition in the visual cortex begins at eye opening. Nat Neurosci. 2007; 10:370–375. [PubMed: 17293862]

Southwell DG, Froemke RC, Alvarez-Buylla A, Stryker MP, Gandhi SP. Cortical plasticity induced by inhibitory neuron transplantation. Science. 2010; 327:1145–1148. [PubMed: 20185728]

Sternson SM, Roth BL. Chemogenetic tools to interrogate brain functions. Annu Rev Neurosci. 2014; 37:387–407. [PubMed: 25002280]

Sugiyama S, Di Nardo AA, Aizawa S, Matsuo I, Volovitch M, Prochiantz A, Hensch TK. Experience-dependent transfer of Otx2 homeoprotein into the visual cortex activates postnatal plasticity. Cell. 2008; 134:508–520. [PubMed: 18692473]

Tamura H, Kawata M, Hamaguchi S, Ishikawa Y, Shiosaka S. Processing of neuregulin-1 by neuropsin regulates GABAergic neuron to control neural plasticity of the mouse hippocampus. J Neurosci. 2012; 32:12657–12672. [PubMed: 22972991]

Tropea D, Kreiman G, Lyckman A, Mukherjee S, Yu H, Horng S, Sur M. Gene expression changes and molecular pathways mediating activity-dependent plasticity in visual cortex. Nat Neurosci. 2006; 9:660–668. [PubMed: 16633343]

Vullhorst D, Neddens J, Karavanova I, Tricoire L, Petralia RS, McBain CJ, Buonanno A. Selective expression of ErbB4 in interneurons, but not pyramidal cells, of the rodent hippocampus. J Neurosci. 2009; 29:12255–12264. [PubMed: 19793984]

Wen L, Lu YS, Zhu XH, Li XM, Woo RS, Chen YJ, Yin DM, Lai C, Terry AV Jr, Vazdarjanova A, et al. Neuregulin 1 regulates pyramidal neuron activity via ErbB4 in parvalbumin-positive interneurons. Proc Natl Acad Sci U S A. 2010; 107:1211–1216. [PubMed: 20080551]

Woo RS, Li XM, Tao Y, Carpenter-Hyland E, Huang YZ, Weber J, Neiswender H, Dong XP, Wu J, Gassmann M, et al. Neuregulin-1 enhances depolarization-induced GABA release. Neuron. 2007; 54:599–610. [PubMed: 17521572]

Xu X, Olivas ND, Ikrar T, Peng T, Holmes TC, Nie Q, Shi Y. Primary visual cortex shows laminar specific and balanced circuit organization of excitatory and inhibitory synaptic connectivity. J Physiol. 2016

Xu X, Roby KD, Callaway EM. Immunochemical characterization of inhibitory mouse cortical neurons: three chemically distinct classes of inhibitory cells. J Comp Neurol. 2010; 518:389–404. [PubMed: 19950390]

Zhou P, Zhang Y, Ma Q, Gu F, Day DS, He A, Zhou B, Li J, Stevens SM, Romo D, et al. Interrogating translational efficiency and lineage-specific transcriptomes using ribosome affinity purification. Proc Natl Acad Sci U S A. 2013; 110:15395–15400. [PubMed: 24003143]

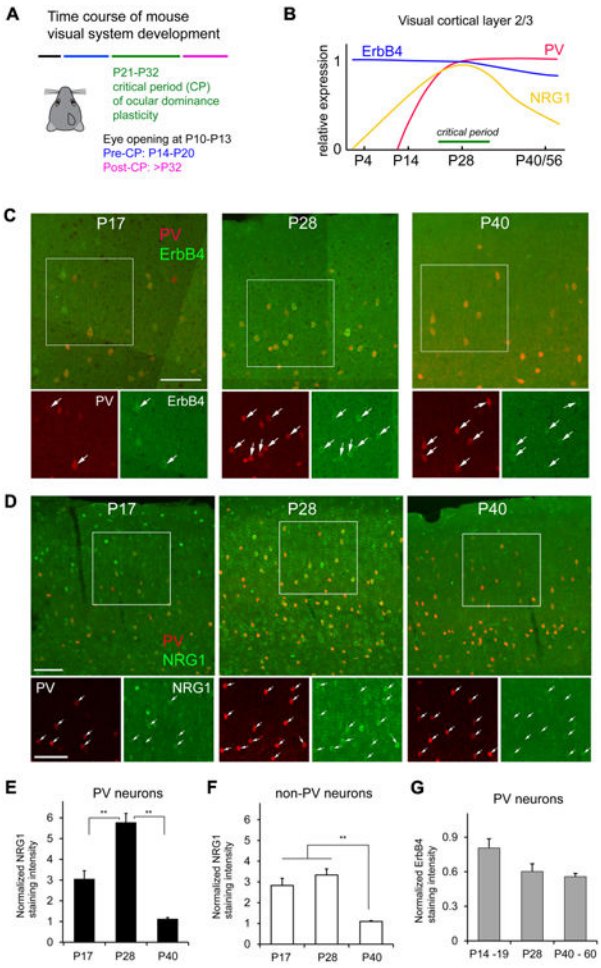

Figure 1. NRG1 and ErbB4 expression in PV neurons is developmentally regulated

A, The developmental times for mouse eye opening; before, during and after the critical period (CP) for ocular dominance plasticity (Smith and Trachtenberg, 2007). **B**, A summary diagram for NRG1, ErbB4 and PV expression levels in mouse visual cortex L2/3 from P0 to P56 compared with the critical period for ocular dominance plasticity. The diagram is constructed based on our immunostaining data and *in situ* gene hybridization data from the Allen Brain Atlas. **C**, Representative confocal images of PV expression (red) and ErbB4 immunolabeling (green) in PV-Cre;Ai9 mouse sections of postnatal days (P) 17, P28 and P40 (dual overlap in larger upper panel, detailed single label images in smaller lower panels). **D**, Representative confocal images show that NRG1 expression varies in PV cells in PV-Cre;Ai9 mouse V1 before (P17), at the peak of (P28) and after (P40) the critical period (dual overlap in larger upper panel, detailed single label images in smaller lower panels). For both (**C**) and (**D**), the arrows indicate PV cells (red) and their corresponding ErbB4/NRG1 immunolabeling (green). Scale bar = 100 μm. **E**, A bar graph shows that the average strength of NRG1 expression in PV cells varies across P17, P28 and P40, and peaks at P28. The NRG1 staining intensity at different age groups was normalized to the staining intensity of P40 in the staining series. Please see the Methods for quantification and normalization of immunostaining intensity; the overall normalized values from different mice were compared

across different age groups or conditions. PV cell measurements were obtained from 5 different mice for each age group. **, $p < 0.01$ (Non-parametric one-way ANOVA Kruskal Wallis test, followed by Mann–Whitney U tests). **F**, A bar graph shows that average NRG1 expression of non-PV neurons is stronger in earlier ages (i.e., P17 and P28) and then decreases (P40). Non-PV cell measurements were obtained from sections of the same 5 mice for each age group used for PV cell measurements. **, $p < 0.01$. **G**, A bar graph shows the average ErbB4 expression strength across P14-19, P28 and P40. The ErbB4 staining intensity of PV neurons at different age groups (n = 5, 3 and 3 mice, respectively) was normalized to the staining intensity of P40 in the staining series. There appears to be a trend for decreased ErbB4 expression in older ages, but does not reach statistical significance (Kruskal Wallis test, $p = 0.07$).

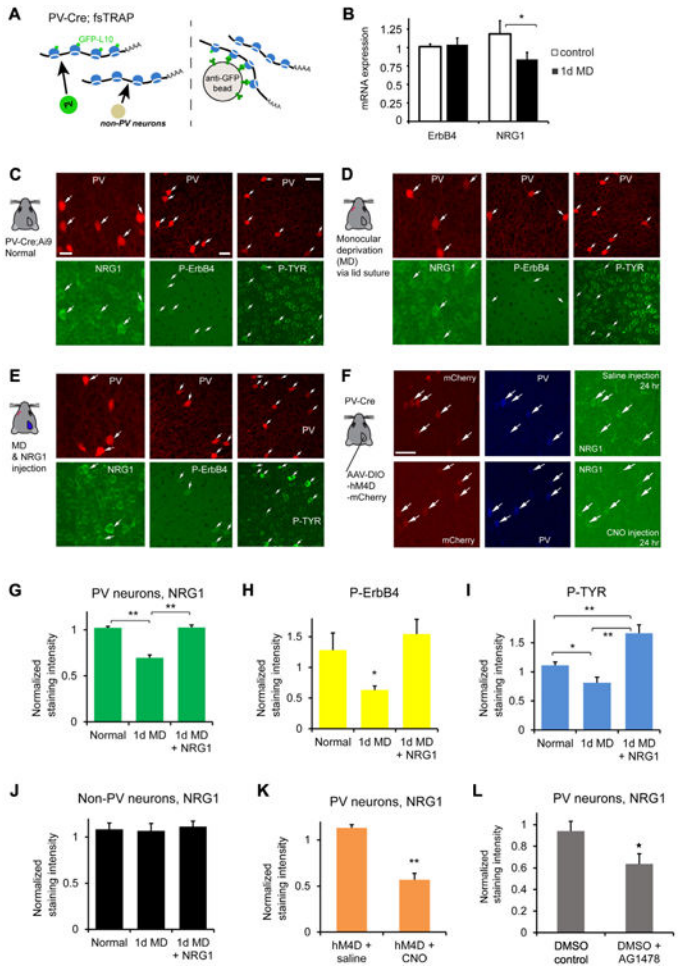

Figure 2. Monocular deprivation rapidly down regulates NRG1/ErbB4 signaling in parvalbumin (PV)-expressing neurons of visual cortex during the critical period of ocular dominance plasticity

A-B, PV cell-specific NRG1/ErbB4 mRNA expression analysis. (**A**) Schematic of the translating ribosome affinity purification (TRAP) strategy (Zhou et al., 2013). Using PV-Cre; fsTRAP mice, translating polyribosomes (polysomes) from PV cells (green cells) have EGFP tags from the EGFP-L10a transgene. Lysis of all cells in the PV-Cre; fsTRAP cortex releases both tagged and nontagged polysomes. Only the tagged polysomes are captured on an anti-GFP affinity matrix, and used for purification of PV-specific mRNA associated with tagged polysomes. See the Methods and Fig. S2 for more information. (**B**) Compared to non-sutured control, 1 day of monocular deprivation (1d MD) reduces NRG1, but not ErbB4 mRNA expression in PV neurons. Each group contained 6-8 samples with each sample that contained 2-3 visual cortex hemispheres. The y axis represents the gene expression level relative to control with the plotted values of $2^{\Delta\Delta Ct}$(Livak and Schmittgen, 2001). *, p = 0.02 (Mann–Whitney U test). **C-E**, Immunochemical analysis of NRG1/ErbB4 signaling. Representative images of NRG1, phospho-specific ErbB4 (P-ErbB4) and phospho-tyrosine (P-TYR) immunostaining are shown for (**C**) PV neurons in the PV-Cre; Ai9 mouse at postnatal day 28, (**D**) after 1 day of monocular deprivation (1d MD), and (**E**) after 1d MD with NRG1 injections [3 times (3×) daily, 0.5 μg NRG1 per mouse]. The image panels are

contrast enhanced for the display, but not for quantitative analysis. The arrows indicate tdTomato+ PV cells (red) and their corresponding immunolabel (green). Scale bar = 20 μm (c, left), 20 μm (c, middle) and 40 μm (c, right). **F**, Reduced PV neuronal activity evoked by DREADDs causes decreased NRG1 expression. Representative images of mCherry label, PV and NRG1 immunostaining in cortical sections of PV-Cre mice with AAV-DIO-hM4D-mCherry expression in binocular V1 with saline control (top row) and clozapine N-oxide (CNO) (bottom row) i.p. injection for 24 hours. G-I, Quantitative assessment of NRG1, P-ErbB4 and P-TYR immunostaining signals in L2/3 PV cells of binocular V1 with and without 1 d MD, and 1 d MD + NRG1. A bar graph in (**G**) shows that the average NRG1 immunostaining signal in L2/3 PV cells significantly differs following 1 d MD but does not differ between control and 1 d MD + NRG1. PV cell measurements in (**G-I**) were obtained from 4-6 different mice for each condition. **, $p < 0.01$ (Kruskal Wallis test, followed by Mann–Whitney U tests). On average, 1d MD PV cells express significantly less NRG1 signal (67.9%) relative to normal control; PV cells of 1d MD occluded by NRG1 injections express similar levels of NRG1 signal relative to control. A bar graph in (**H**) shows average P-ErbB4 immunostaining signal in L2/3 PV cells across different conditions. PV cell measurements were obtained from sections of 3-4 different mice for each condition. *, $p = 0.05$. On average, 1d MD PV cells express 49.5%of the P-ErbB4 signal relative to control. A bar graph in (**I**) shows average P-TYR immunostaining signal across different conditions. * and ** correspond to $p = <0.05$ and $p <0.005$.On average, 1d MD PV cells express significantly less P-TYR signal (73%) relative to control; while 1d MD PV cells treated with NRG1 injections express 150% of the P-TYR signal relative to control. **J**, The NRG1 immunostaining levels in L2/3 non-PV cells of binocular V1 does not differ across different conditions (non-PV neurons obtained from 6 mice each). **K**, The average NRG1 immunostaining signals in L2/3 PV cells are significantly lower in V1 cortical sections of PV-Cre mice with reduced PV neuronal activity evoked by DREADDs *in vivo* via CNO injection, compared to control saline injection (PV neuron measurements obtained from 7 and 5 mice each). **, $p < 0.005$ (Mann–Whitney U test). **L**, Compared to control, the average NRG1 levels in L2/3 PV cells are significantly lower in the non-deprived mouse cortex treated with an ErbB receptor tyrosine kinase inhibitor AG1478 following acute intracerebroventricular delivery (< 24 hr). PV neuron measurements were obtained from 6 mice each. *, $p = 0.04$ (Mann–Whitney U test).

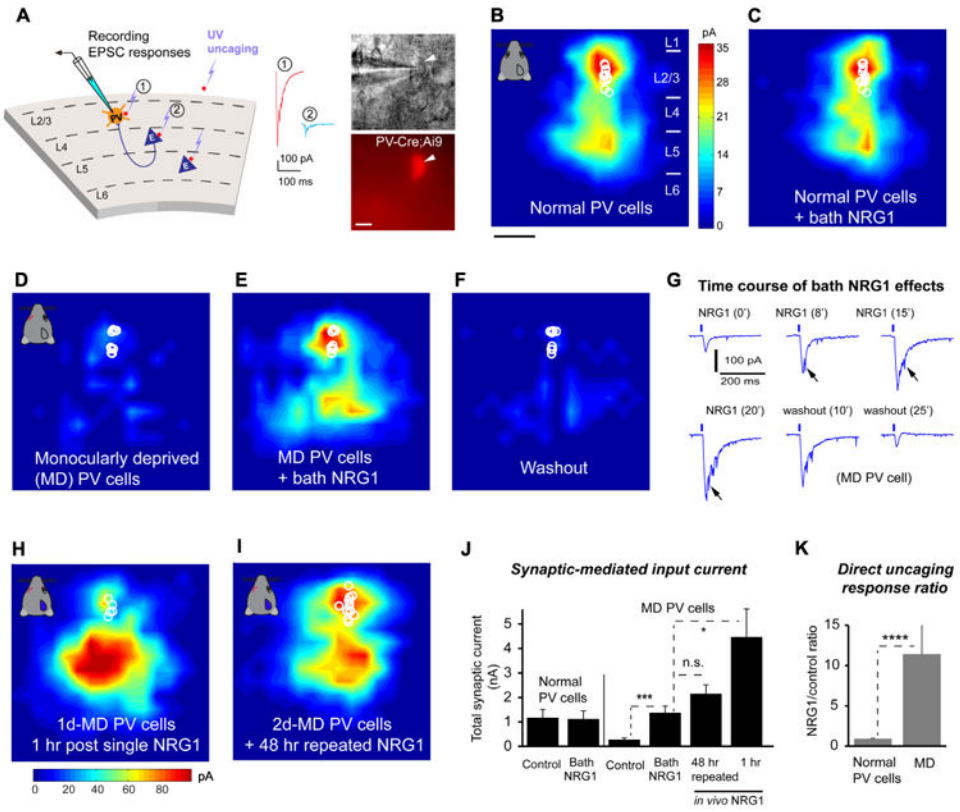

Figure 3. NRG1 treatment rapidly and robustly increases excitatory synaptic input onto monocular deprived PV neurons during the critical period

A, Left: Schematic of laser scanning photostimulation (LSPS) mapping of local synaptic connections to individually recorded PV neurons in V1 slices. Right: targeted recordings of PV neurons are facilitated by tdTomato expression in PV-Cre; Ai9 mouse slices. Scale = 10 μm. LSPS maps the broad spatial pattern of synaptic inputs for the neuron of interest that distinguishes direct uncaging responses (1, red) to assess glutamate mediated excitability/ responsiveness at perisomatic locations, and synaptically mediated responses (2, cyan) to assess circuit inputs from presynaptic neuronal spiking. Cortical layers of 1, 2/3, 4, 5 and 6 in the brain slice are indicated as L1, L2/3, L4, L5 and L6. **B-C**, Acute bath application of NRG1 (5 nM) does not significantly modulate local excitatory synaptic inputs and glutamate mediated excitability of normal PV neurons in non-deprived binocular V1 of control mice. Group-averaged, excitatory input maps of L2/3 PV cells (n = 13 cells) are shown for before (**B**) and during bath NRG1 (20 minutes after NRG1 application) (**C**). White circles represent individual PV neurons. The color scale (**B**) codes integrated excitatory input strength (blue = low, red = high) and applies to all other maps except **H**. The spatial scale beneath (**B**) indicates 200 μm. PV neurons in mice with 1-2 days of monocular lid suture show dramatically lower excitatory synaptic inputs compared to controls (**D**, n = 10 cells). However, excitatory inputs to PV neurons in these deprived mice are restored to levels above that of controls by acute bath application of NRG1 (**E**). This restoration is eliminated by washout of bath NRG1 (**F**). **G**, The fast time course of NRG1 induced potentiation of PV neuronal responses is shown for a representative neuron from a monocular deprived animal. The glutamate uncaging responses were recorded from a deprived PV neuron at a

perisomatic region. Arrows indicate the enhanced magnitude of synaptic inputs superimposed on the larger waveform of the co-enhanced direct response with bath NRG1. **H**, Single *in vivo* NRG1 injection (subcutaneous, 1 μg per mouse) clearly potentiates excitatory input to 1-day monocular deprived PV cells (n = 5 cells) in the slices prepared one hour post injection. The color scale beneath (**H**) codes integrated excitatory input strength. Note that compared to bath NRG1, *in vivo* NRG1 causes larger direct responses that mask some of the smaller synaptic inputs from perisomatic regions in L2/3. This contributes to the appearance that enhancement of excitatory inputs from deep layers by *in vivo* NRG1 is stronger than those from layer 2/3 (cf. Fig. 3E and H), however this is probably due to the relatively larger concentration of NRG1 required for the *in vivo* experiments. **I**, 2-day NRG1 injections (0.5 μg every 8 hours) during 2d MD *in vivo* prevent excitatory input reduction. Note that injecting NRG1 for only the first day of 2d MD does not prevent excitatory input reduction. Group-averaged, excitatory input maps are shown for L2/3 PV cells for 2d MD mice with 2-day NRG1 injections (n = 10 cells). **J**, Summary data of average total synaptic input strength measured for L2/3 PV neurons under the specified conditions. * and ***, p = 0.03 and 0.001 (Mann–Whitney U tests). The n.s. indicates no significant difference (p = 0.2). **K**, Direct uncaging response ratios of before and during bath NRG1 for normal versus deprived PV cells. We measured peak direct responses, which are not affected by overriding synaptic inputs.****, p = 4.6E-05 (Mann–Whitney U test).

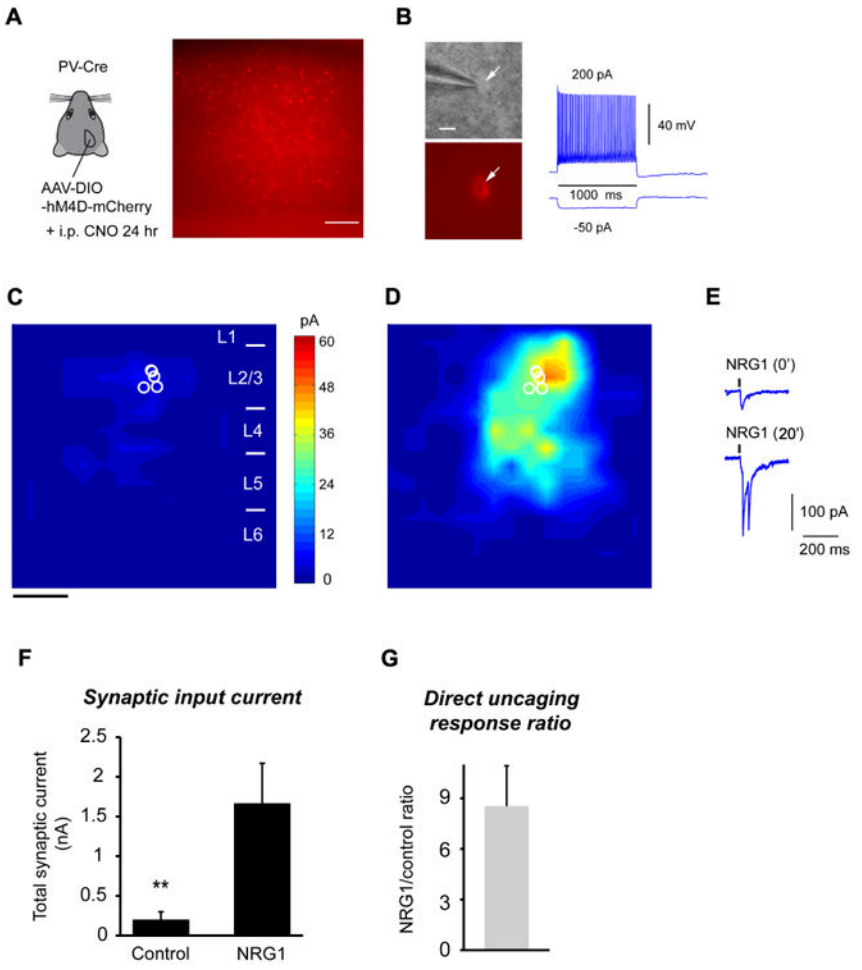

Figure 4. *In vivo* inactivation of PV neurons by DREADDs for 24 hours shows a large reduction in local excitatory input, and this is restored by bath NRG1 application

A, Use of the DREADDS to reduce PV neuron activity *in vivo*, phenocopies the effect evoked by monocular deprivation. Left, a schematic of injecting AAV-DIO-hM4D-mCherry in binocular V1 of the PV-Cre mouse. Right, a representative slice image showing AAV labels by mCherry visualization in PV neurons. Scale = 200 μm. **B**, Left: Targeted recordings of PV neurons are facilitated by mCherry expression in PV-Cre mouse slices. Right: *In vivo* CNO treatment does not affect the general fast-spiking phenotype of PV neurons in *in vitro* recordings. Scale = 10 μm. **C-D**, Group-averaged, excitatory input maps of L2/3 PV cells (n = 6 cells) are shown for before (**C**) and during bath NRG1 (**D**). The spatial scale beneath (**C**) indicates 200 μm. **E**, example responses evoked by photostimulation in the same perisomatic site before and during bath NRG1. **F**, Summary data of average total synaptic input strength measured for L2/3 PV neurons before (control) and during bath NRG1. **, $p < 0.01$ (Mann–Whitney U test). **G**, Direct uncaging response ratio of during bath NRG1 for DREADDs-inhibited PV cells versus before NRG1 application.

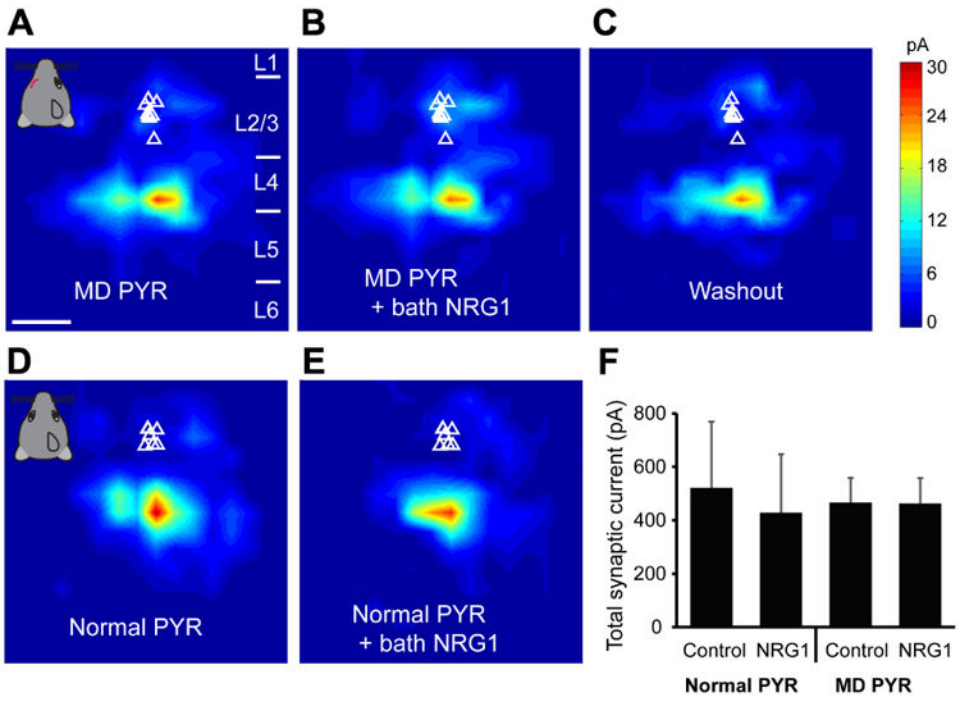

Figure 5. NRG1 treatment does not modulate excitatory synaptic input onto pyramidal neurons under normal or monocular deprivation conditions

A-C, Quantitative group-averaged, excitatory input maps of monocular deprived (MD) L2/3 pyramidal (PYR) neurons are shown for before (**A**, n = 9 cells), during (20 minutes after NRG1 application, **B**) and after washout (**C**) of bath NRG1. White triangles represent individual pyramidal neurons. The spatial scale bar in (**A**) indicates 200 μm. Color scale in (**C**) indicates excitatory input strength. Cortical layers of 1, 2/3, 4, 5 and 6 in the brain slice are indicated as L1, L2/3, L4, L5 and L6. **D-E**, Group-averaged, excitatory input maps of normal L2/3 pyramidal neurons are shown for before (**D**, n = 6 cells) and during bath NRG1 (**E**). **F**. Summary data of average total synaptic input strength measured for control (n = 6) versus deprived (n = 9) L2/3 pyramidal neurons. There is no significant difference between the groups ($p > 0.5$, Mann–Whitney U tests).

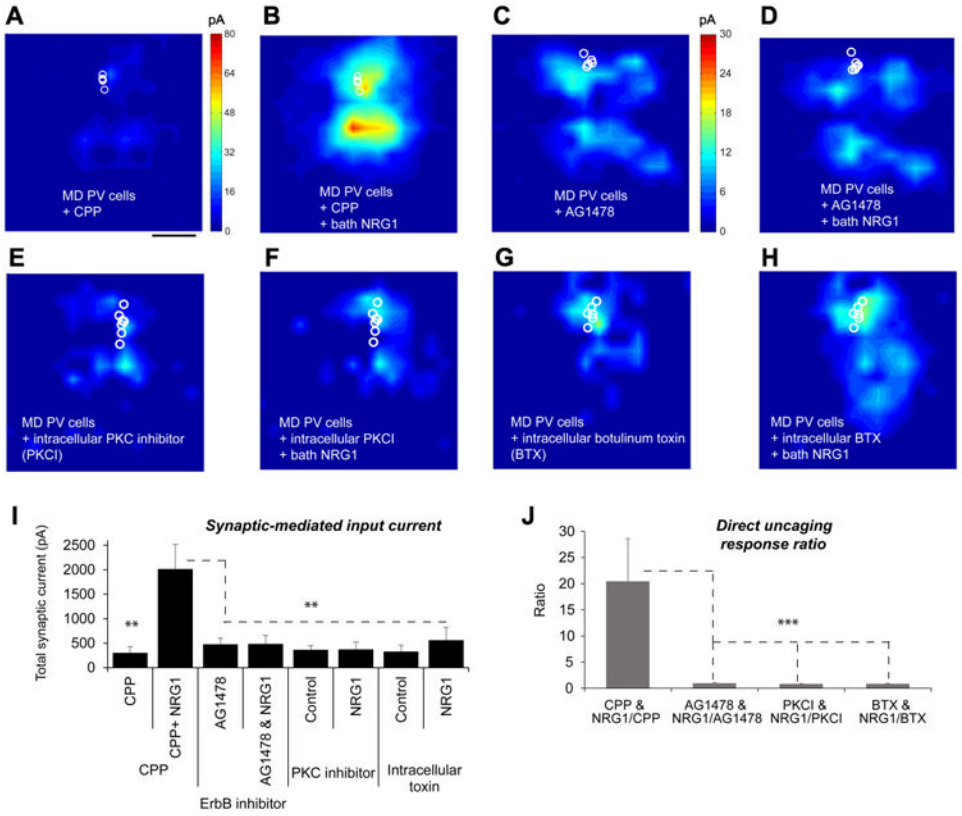

Figure 6. NRG1/ErbB4 downstream signaling requires PKC dependent activation and membrane fusion–dependent exocytosis of AMPA receptors to restore excitatory inputs to deprived PV neurons

A-B, The presence of a NMDAR antagonist, CPP (3-((R)-2-carboxypiperazin-4-yl)-propyl-1-phosphonic acid) does not affect NRG1 potentiation of excitatory inputs of 1-2 day deprived PV neurons. Group-averaged, excitatory input maps of L2/3 PV cells (n = 5 cells) in the CPP presence are shown for before (**a**) and during bath NRG1 (**B**). The spatial scale beneath (**A**) indicates 200 μm. **C-D**, An ErbB receptor tyrosine kinase inhibitor, AG1478 blocks NRG1 effects on 1-2 day deprived PV cells. Group-averaged, excitatory input maps of L2/3 PV cells (n = 10 cells) in the presence of AG1478 are shown for before (**C**) and during bath NRG1 (**D**). **E-F**, Intracellular application of a pseudosubstrate peptide inhibitor of protein kinase C (PKC (19-36), PKCI) prevents NRG1 induced effects on the recorded deprived PV cells. Group-averaged, excitatory input maps of L2/3 PV cells (n = 8 cells) in the intracellular presence of PKC (19-36) are shown for before (**E**) and during bath NRG1 (**F**). **G-H**, Intracellular application of botulinum toxin light chains (BTX) largely prevents NRG1 induced effects on the recorded deprived PV cells. Group-averaged, excitatory input maps of L2/3 PV cells (n = 7 cells) in the intracellular presence of BTX are shown for before (**G**) and during bath NRG1 (**H**). **I**, Summary data of average total synaptic input strength measured for L2/3 PV neurons under the specified conditions. ** indicate the significance levels of $p < 0.01$ (Mann–Whitney U tests). **J**, Direct uncaging response ratios of before and during bath NRG1 measured for L2/3 deprived PV neurons under the specified conditions. ***, $p < 0.001$ (Mann–Whitney U test).

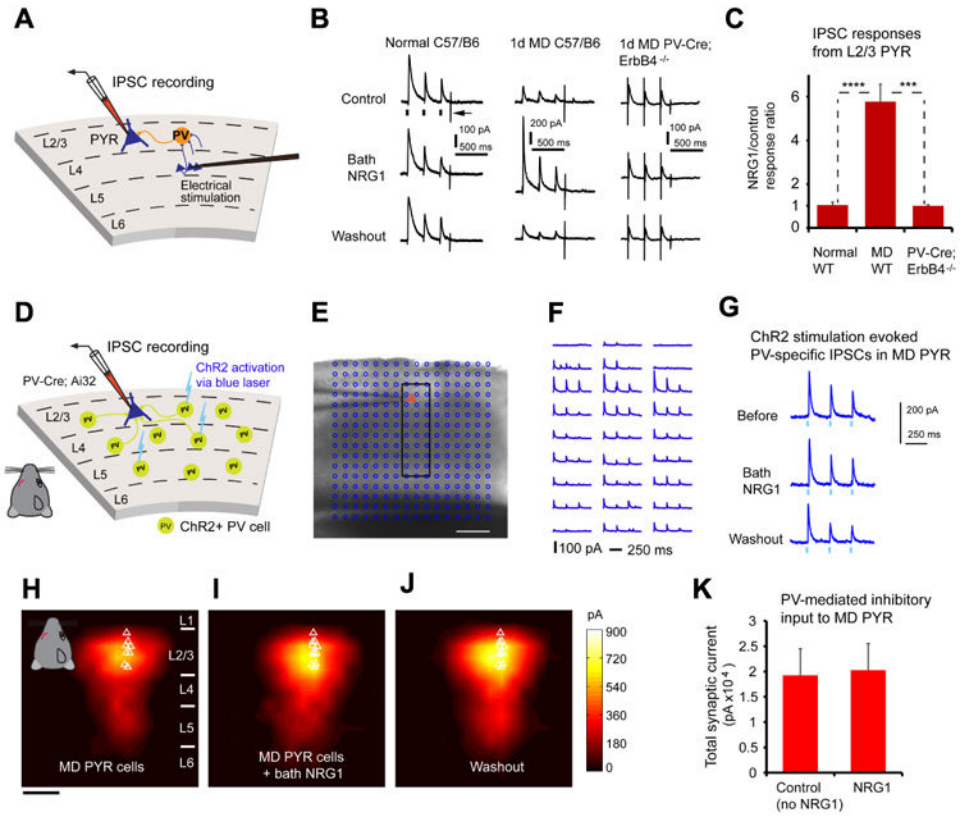

Figure 7. During critical period monocular deprivation, NRG1 enhances evoked synaptic inhibition onto pyramidal neurons without altering the strength of PV inhibitory synaptic connections to pyramidal neurons

A, Schematic of recording inhibitory postsynaptic current (IPSC) responses in L2/3 pyramidal (PYR) neurons by preferentially activating L4->L2/3 feedforward projections to L2/3 PV neurons through L4 electrical stimulation. **B-C**, Bath NRG1 increases evoked IPSCs to monocular deprived (MD)pyramidal neurons in slices of wild type C57/B6 mice (n = 16 cells), but not normal pyramidal neurons (n = 6 cells), or pyramidal neurons (n = 5 cells) in slices of PV-Cre; ErbB4$^{flx/flx}$ mice. For each trial, electrical stimulation (1 ms, 20 μA) was applied three times (represented by three black ticks beneath one example trace in **B**).For the example trace, the arrow indicates the current injection response to monitor access resistance during the experiment. ***, and ****, p = 0.003 and 6.1E-04 (Mann–Whitney U tests). **D-K**, The responsiveness of PV inhibitory input connections to deprived pyramidal neurons is not modulated by bath NRG1, as assessed with optogenetically evoked PV inhibitory inputs. **D**, Schematic of mapping PV inhibitory IPSCs to individually recorded L2/3 pyramidal neurons in local V1 circuits in PV-Cre;Ai32 mouse slices. **E**, A representative mapping grid with ChR2 photoactivation sites (cyan circles) is superimposed to the slice image, and ChR2-evoked IPSC responses from the rectangular region in **E** to the recorded pyramidal neuron are shown in **F**. **G**, Example IPSC responses recorded from the pyramidal neuron shown in (**E, F**) while directly activating ChR2-expressing PV cells through optogenetic stimulation in one map location before, during and after washout of bath NRG1. The repeated blue laser flashes (0.25 ms) (represented by three blue ticks beneath the traces in **G**) were applied to each map location. Group-averaged, inhibitory

input maps of L2/3 pyramidal neurons are shown for **H**, before (n = 11 cells) and **I**, during bath NRG1 (20 minutes after NRG1 application) and **J**, after washout of bath NRG1. White triangles represent individual pyramidal neurons. Color scale (**J**) indicates integrated PV inhibitory input strength (black = low, yellow = high). **K**, Summary data of average total synaptic input strength measured for deprived L2/3 pyramidal neurons (n = 11) for control and bath NRG1. The spatial scale bars in (**E**, **H**) indicate 200 μm. There is no significant difference between the groups (p = 0.7, Mann-Whitney U test).

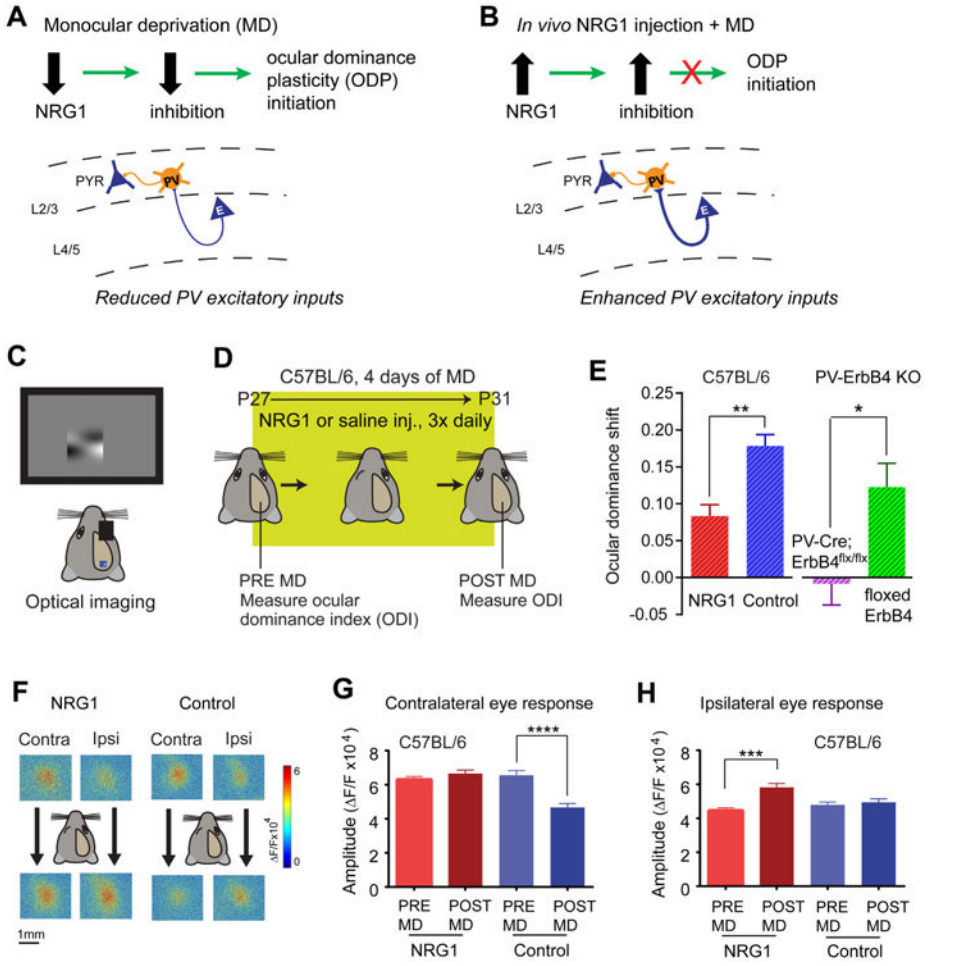

Figure 8. Alteration of NRG1/ErbB4 signaling in PV neurons *in vivo* suppresses critical period ocular dominance plasticity

A-B, Schematic of our model. **A**, Monocular deprivation (MD)-induced reduction of NRG1 expression and NRG1/ErbB4 signaling in PV-neurons reduces excitatory inputs onto these cells. The subsequent decrease of cortical inhibition is the necessary first step in ocular dominance plasticity (ODP) initiation. **B**, Elevated NRG1 in the cortex enhances excitatory inputs to PV neurons during MD, which occludes the MD-induced reduction of cortical inhibition and suppresses ODP during the normal critical period. **C-E**, The reduction in ocular dominance shift observed after NRG1 treatment during the critical period reflects a suppression of ODP. Illustration of the experimental paradigm (**C, D**) for assessing ocular dominance in wild type C57BL/6 mice before and after 4 days of MD during the critical period. **E**, Ocular dominance shift is reduced in NRG1 treated critical period animals (n = 6, red) compared with control critical period animals (n = 7, blue). **, p = 0.004 (Mann-Whitney U test). Plasticity is also reduced in PV-specific ErbB4 knockout (KO) animals (PV-Cre; ErbB4$^{flx/flx}$, n = 6, purple) compared with their ErbB4 $^{flx/flx}$ littermates (n = 8, green). *, p = 0.014 (Mann-Whitney U test). **F**, Examples of contralateral and ipsilateral visual response maps from an NRG1 treated animal (left) and a control animal (right)before (top panels) and after (bottom panels) 4 days of MD. While deprivation causes a loss of contralateral deprived eye input in normal mice, it causes non-deprived ipsilateral eye gain

in NRG1 treated animals. **G**, Contralateral (deprived) input changes for control: pre-MD (n = 7 mice, 24 responses) versus post-MD (n = 7 mice, 23 responses). ****, $p < 0.0001$ (Mann–Whitney U test). No contralateral input change observed in NRG1 treated animals: pre-MD (n = 7 mice, 22 responses) versus post-MD (n = 5 mice, 16 responses). $p = 0.3$ (Mann-Whitney test). **H**, In contrast, ipsilateral input increases in NRG1 treated animals: pre-MD (n= 6 animals, 18 responses) versus post-MD (n=6 mice, 15 responses). *** $p = 0.0002$ (Mann–Whitney U test). No ipsilateral input change observed in control animals: pre-MD (n = 6 animals, 23 responses) versus post-MD (n = 6 animals, 23 responses). $p = 0.6$ (Mann-Whitney test).